

# Competing Electronic Phases in the Topological Crystalline Insulator $\text{Pb}(x)\text{Sn}(1-x)\text{Te}$

Vikram Tripathi

07 November, 2017

## **Co-worker:**

Sarbajaya Kundu (TIFR)

## **Discussions:**

R. Sensarma (TIFR)

K. Damle (TIFR)

## **Funding:**

Department of Science and Technology, India

## **Refs.:**

ArXiv:1704.07437 (to appear in PRB)

ArXiv:1709.02322

# Outline

- Topological concepts in condensed matter
- $Z_2$  topological insulators
- Topological crystalline insulators (TCIs)
- Electron correlations (parquet RG analysis)
- Possible instabilities

# What is topology?

Loose definition:

A mathematical concept dealing with properties that remain unchanged under smooth, local deformations.

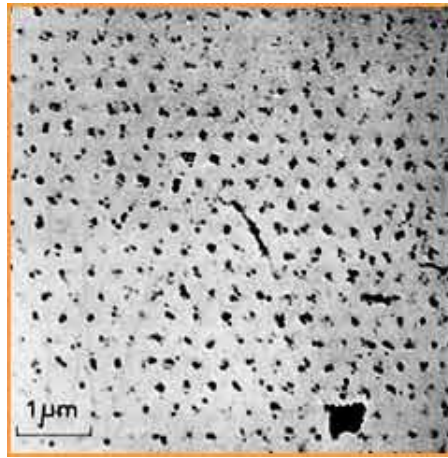
A donut and a teacup have the same number of “handles” or topology.



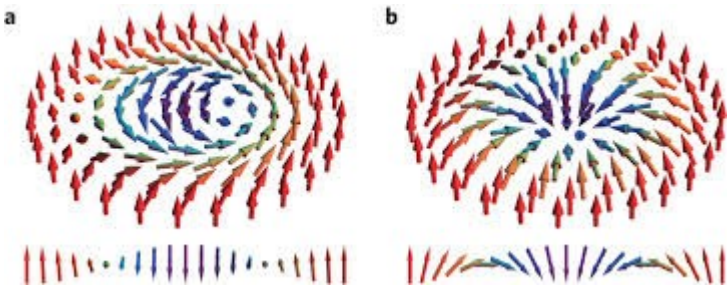
# Examples of topological structures



Screw dislocation  
in a wall.



First image of Abrikosov vortex lattice in superconductor, 1967. Phase of the Cooper-pair wave function rotates by  $2\pi n$  as one circles a vortex. Continuity then requires the vorticity  $n$  to be an integer.



$$\mathbf{M}(x, y) = (\sin(\Theta(r)) \cos(\Phi(\varphi)), \sin(\Theta) \sin(\Phi), \cos(\Theta)),$$

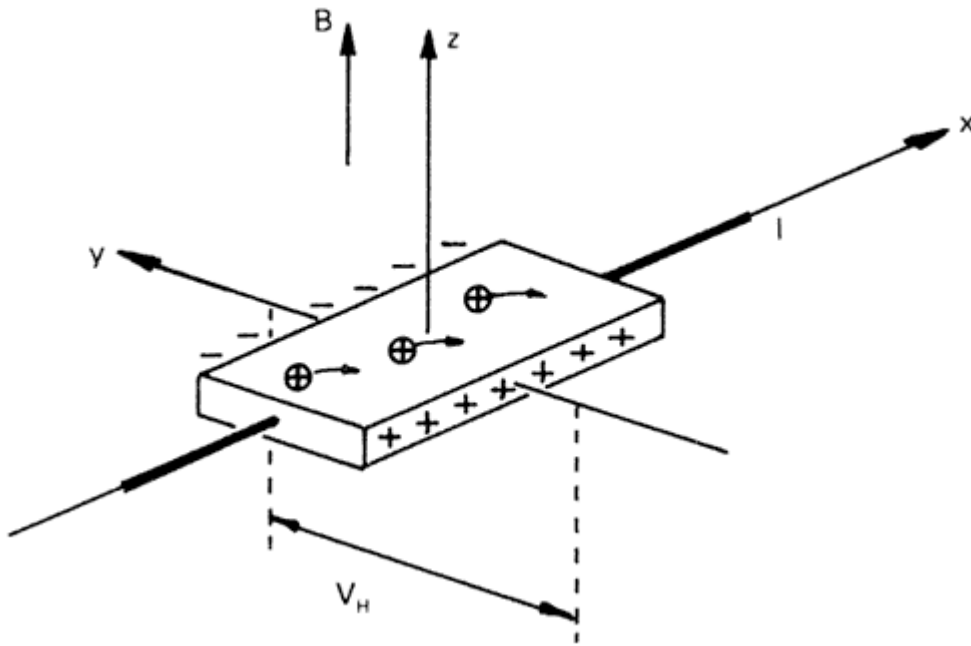
$$\Phi = m\varphi + \gamma$$

$$n = \frac{1}{4\pi} \int dx dy \mathbf{M} \cdot \partial_x \mathbf{M} \times \partial_y \mathbf{M}$$

$$= \frac{1}{4\pi} \int_0^\infty dr \int_0^{2\pi} d\varphi \frac{d\Theta(r)}{dr} \frac{d\Phi(\varphi)}{d\varphi}$$

Skyrmions in 2D magnetic semiconductor  
 $\text{GaV}_4\text{S}_8$ .

# Quantum Hall effect

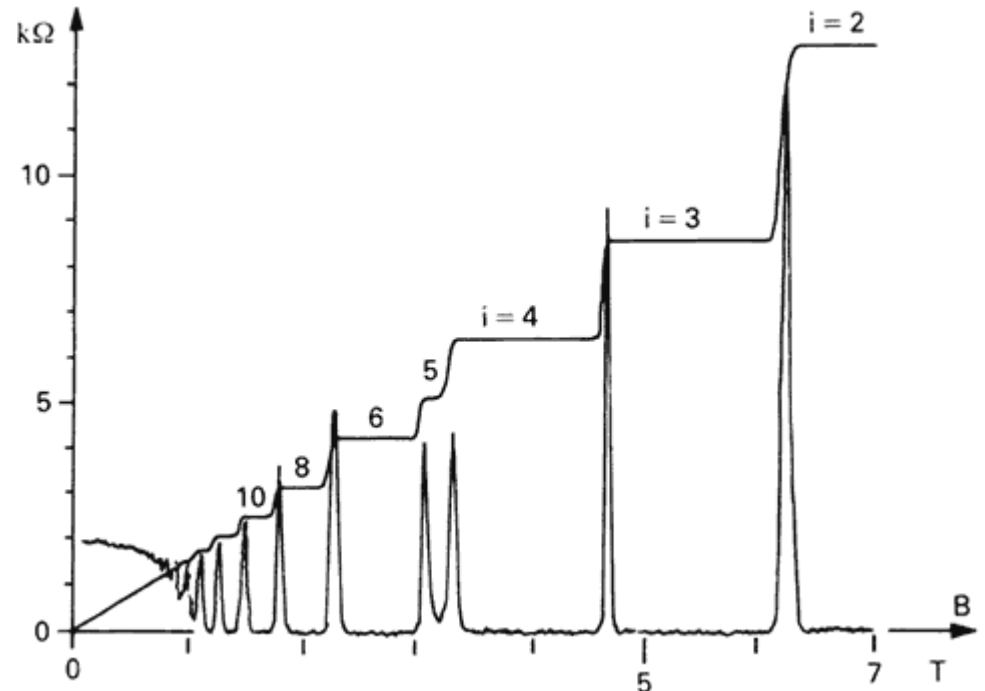


Hall Resistance:  $R_H = \frac{V_y}{I_x B} = \frac{1}{ne}$

From quantum mechanics of particle  
In magnetic field:

$$n = \frac{\nu e}{hB} \Rightarrow R_H = \frac{h}{\nu e^2}$$

(Hall insulator)



# Berry phase

Consider a time-independent Hamiltonian that has some dependence on a parameter. Schrödinger eq. for ground state is

$$H(\xi)|\Psi_0(\xi)\rangle = E_0(\xi)|\Psi_0(\xi)\rangle$$

Define phase difference between the eigenstates at two different parameter values:

$$\exp[-i\Delta\varphi_{12}] = \frac{\langle\Phi_0(\xi_1)|\Phi_0(\xi_2)\rangle}{|\langle\Phi_0(\xi_1)|\Phi_0(\xi_2)\rangle|} \Rightarrow \Delta\varphi_{12} = -\text{Im} \ln(\langle\Phi_0(\xi_1)|\Phi_0(\xi_2)\rangle)$$

Berry phase is the total phase accumulated over a closed path in parameter space:

$$\gamma = \Delta\varphi_{12} + \Delta\varphi_{23} + \dots + \Delta\varphi_{N,1}$$

# Berry connection and curvature

The continuous form looks nicer and allows us to introduce a fictitious vector potential, the Berry connection:

$$\gamma = \oint_C \mathbf{A}(\boldsymbol{\xi}) \cdot d\boldsymbol{\xi}$$

$$\mathbf{A}(\boldsymbol{\xi}) = -\text{Im} \langle \Psi_0(\boldsymbol{\xi}) | \nabla_{\boldsymbol{\xi}} \Psi_0(\boldsymbol{\xi}) \rangle$$

The line integral is identified as a flux enclosed by closed path C. Similarly to electromagnetism, using “Stokes’ theorem”, we identify a fictitious magnetic field, the Berry curvature:

$$\Omega_{\alpha\beta} = -2 \text{Im} \langle \partial_{\alpha} \Psi_0(\boldsymbol{\xi}) | \partial_{\beta} \Psi_0(\boldsymbol{\xi}) \rangle$$

If C is a curve on a closed surface, then the Berry phase is not uniquely determined since C could be the boundary of two possible surfaces now. However, the difference is  $2\pi$  and unique.

# The Chern number in a crystal

Instead of the polar and azimuthal angles of the last example, the corresponding parameter is now the momentum. In 2D, for example,

$$C_1 = \frac{1}{2\pi} \int_{\text{BZ}} d\mathbf{k} \Omega(\mathbf{k}) = -\frac{1}{\pi} \int_{\text{BZ}} d\mathbf{k} \sum_n \text{Im} \langle \partial_1 u_{j\mathbf{k}} | \partial_2 u_{j\mathbf{k}} \rangle$$

This is the so-called first Chern number, and is an integer.

# Quantum Hall effect, topological band theory

D. J. Thouless, M. Kohmoto, M. P. Nightingale, and M. Den Nijs  
*Quantized Hall conductance in a two-dimensional periodic potential.*  
Physical Review Letters, **49**(6):405, 1982.

Using linear response theory, TKNN showed  $\sigma_{xy} = \frac{e^2}{h} C_1$

If the Chern number is zero, then we are looking at a normal band insulator.

If nonzero, then the bandstructure has nontrivial topology  
- this is a **Chern insulator**. TKNN showed that by using the actual Landau level wavefunctions, the Chern number is one for each occupied Landau level.

The Chern insulator thus has a finite and quantized Hall resistance.

The great importance of the Thouless et al. result is that it opens up the possibility of having a Hall conductance quantization even in the absence of time-reversal symmetry breaking.

# Hall quantization without Landau levels

F.D.M. Haldane

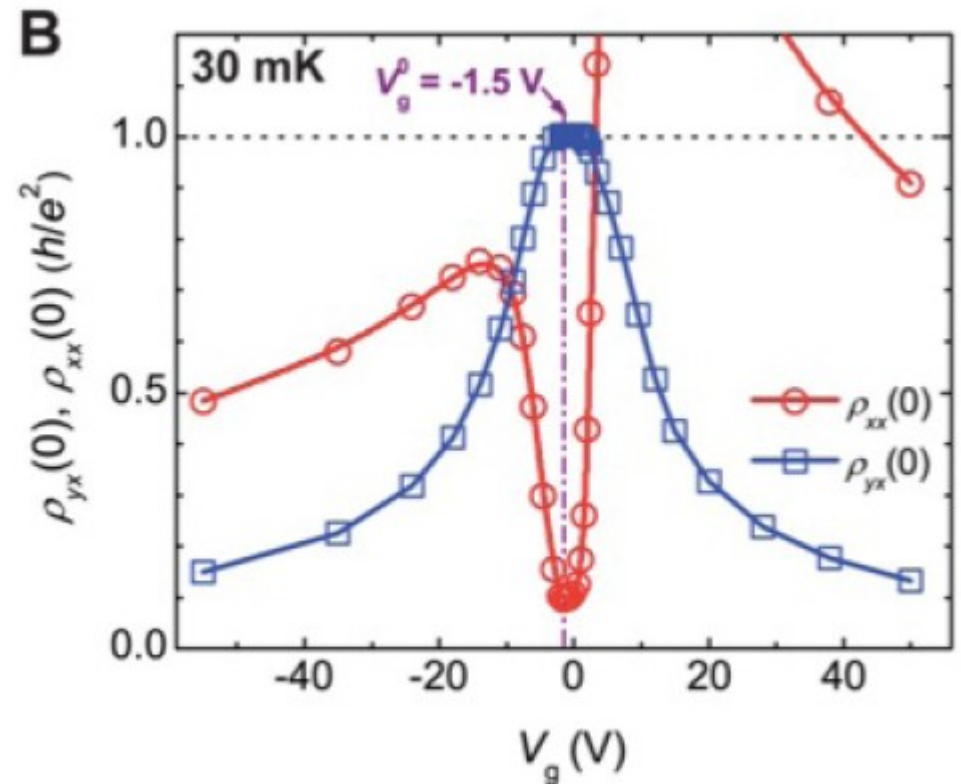
*Model for a Quantum Hall Effect without Landau Levels: Condensed-Matter Realization of the "Parity Anomaly".*

Physical Review Letters, **61**(18):2015, 1988.

Haldane constructed a simple (graphene) lattice model with nearest and next-nearest neighbour hopping. Model had broken time-reversal symmetry but zero total magnetic field per hexagon.

No Landau levels. However the two-component Bloch states  $|u(\mathbf{k})\rangle$  have a structure similar to the textbook example of a spin-1/2 particle in a rotating magnetic field.

Experimental evidence of a Chern Insulator  $(\text{Bi,Sb})_2\text{Te}_3$ , Cui-Zu Chang et al., Science, **340**(6129):167–170, 2013.



# $Z_2$ Topological Insulators

C. L. Kane and E. J. Mele, PRL (2005), *ibid.* (2007)

R. Roy, PRB (2009)

Consider two “time-reversed” copies of Haldane-type Chern insulator. Total Chern number is zero, i.e.  $C_1 + C_2 = 0$ .

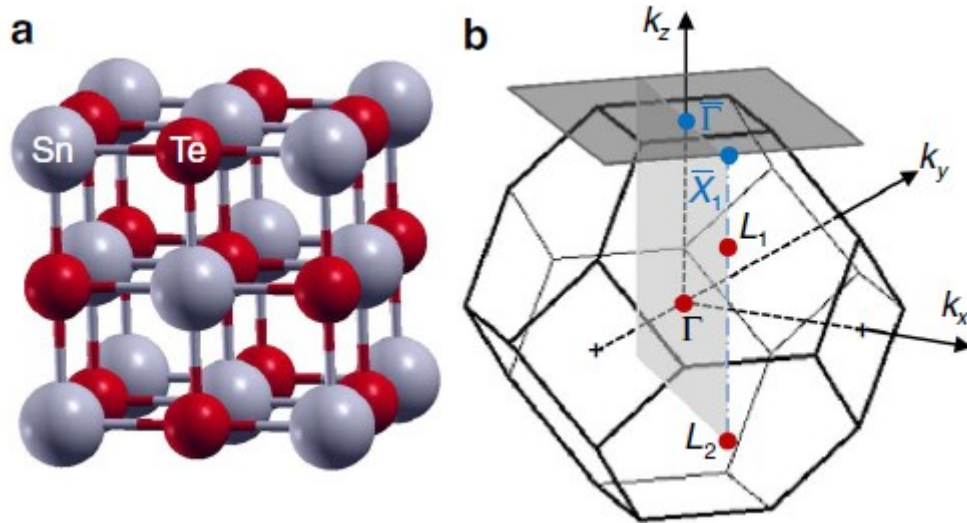
But this could mean either both are zero, or their difference is  $\pm 2$ . If the difference is nonzero, the insulator is topologically nontrivial.

Idea may be extended to 3 dimensions.

# Topological crystalline insulators

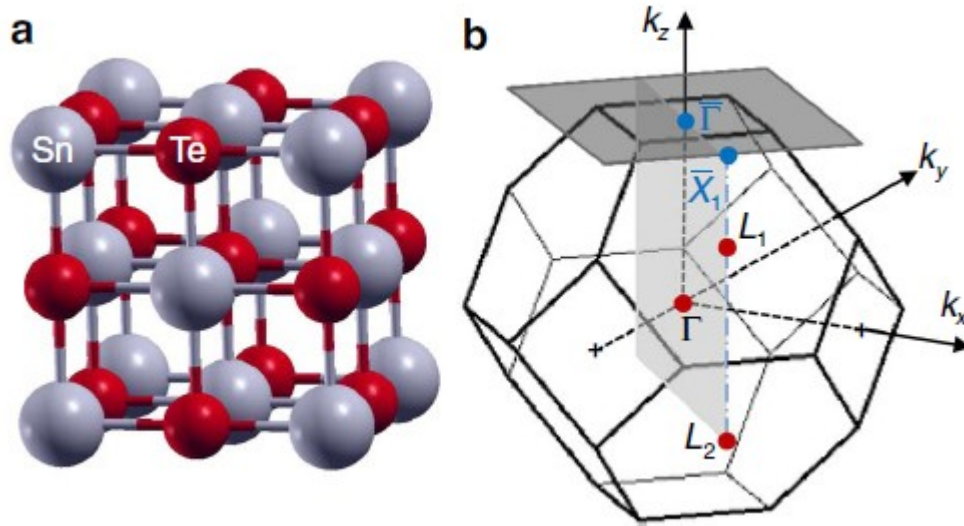
Low energy surface states topologically protected by crystalline symmetry instead of (usual) time reversal symmetry [Fu, PRL (2011)].

Proposed material realization: SnTe  
[Hsieh et al., Nature Comm. (2012)]



Bandgap at L-points  
Inverted wrt PbTe.  
[Dimmock et al., PRL (1966)]

# SnTe as a TCI



Neither PbTe or SnTe are conventional Z2 topological insulators.

Crystal momenta in  $\Gamma L_1 L_2$  are invariant under mirror reflections about (110) plane in real space. Bloch states on this plane can be thus labelled by the eigenvalues  $\pm \iota$  of this mirror reflection operation  $M$ , and associated Chern number  $n_{\pm \iota}$ .

Bandstructure calculations show that the mirror Chern number  $(n_+ - n_-)/2$  is a nonzero integer for SnTe but zero for PbTe.

[Hsieh et al., Nature Comm. (2012)]

# Excitations near the L points

Mitchell & Wallis, Phys. Rev. (1966)

$$H = m\sigma_z + v(k_1s_2 - k_2s_1)\sigma_x + v_3k_3\sigma_y$$

$k_3$  along  $\Gamma L$ ,  $k_1$  along  $[110]$  direction.

Eigenvectors of Pauli matrix  $\sigma_z$  denote p-orbital on cation Pb/Sn (1,0) or anion Te (0,1).

Pauli matrix  $s_3$  denotes angular momentum of electron along  $\Gamma L$  direction.

Positive  $m$  means conduction band at L derived from cation. Reflection about (110) plane denoted by  $M = -\tau s_1$ .

## ... Excitations near the L points

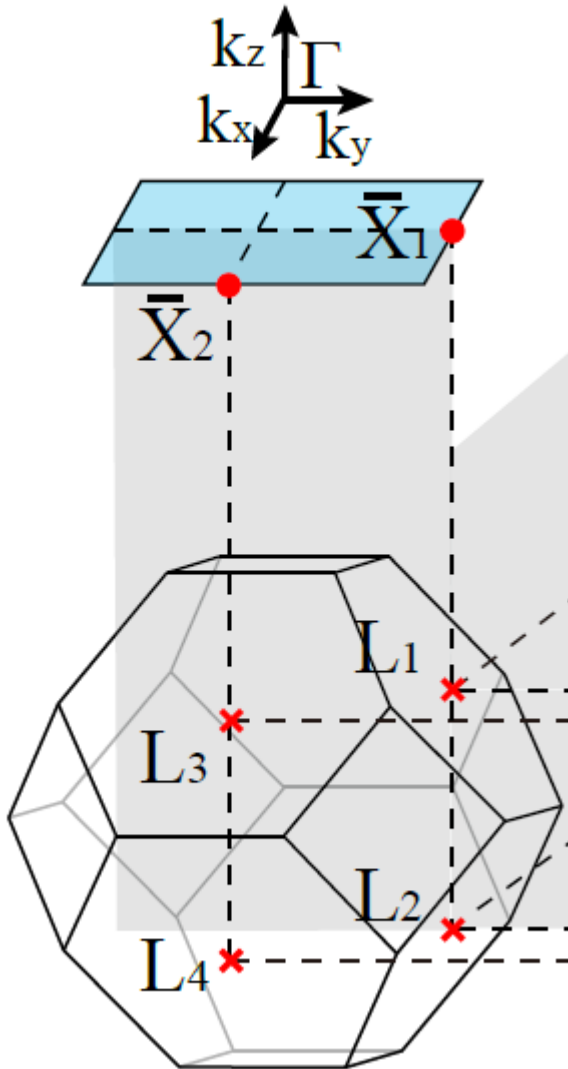
Consider Hamiltonian on mirror invariant plane  $k_1 = 0$ .

$$H_0^\pm = m\sigma_z \mp vk_2\sigma_x + v_3k_3\sigma_y \quad (\text{Massive Dirac fermion})$$

As Sn doping increases, the sign of the mass flips at some value of doping. Chern number changes by  $\pm 1$ . Same thing happens at both L1 and L2 point  $\rightarrow$  Chern number changes by  $\pm 2$ .

Thus either PbTe or SnTe is topologically nontrivial. Bandstructure calculation shows SnTe is topologically nontrivial. [Hsieh et al., Nature Comm. (2012)]

# Effective Hamiltonian at (001) surface



On (001) surface, pairs of  $\bar{L}$  points get projected to a single  $\bar{X}$  point.

Low-energy effective Hamiltonian  
[Liu et al., PRB(R) (2013)]:

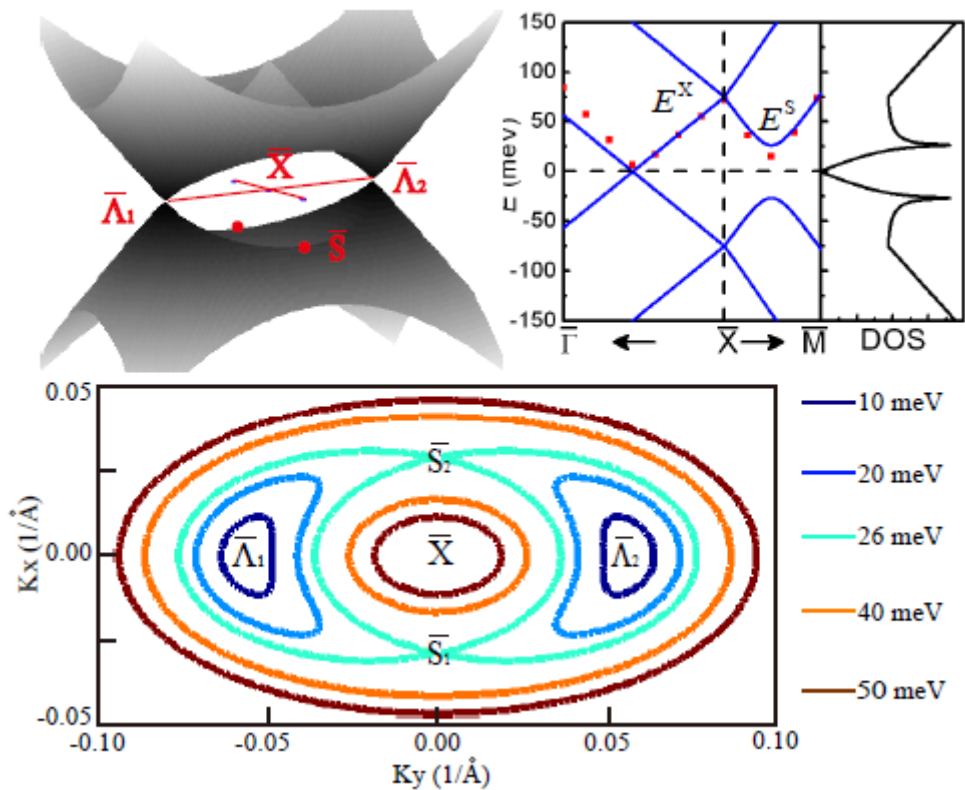
$$H_{\bar{X}_1}(k) = (v_x k_x s_y - v_y k_y s_x) + m\tau_x + \delta s_x \tau_y$$

Here  $\tau$  - Pauli matrix in valley (L) space.  
and  $s$  refers to spin space.

# Bandstructure near $\bar{X}$ point

$$H_{\bar{X}_1}(k) = (v_x k_x s_y - v_y k_y s_x) + m\tau_x + \delta s_x \tau_y$$

$$E_{H,L}(k) = \sqrt{m^2 + \delta^2 + v_x^2 k_x^2 + v_y^2 k_y^2 \pm 2\sqrt{m^2 v_x^2 k_x^2 + (m^2 + \delta^2) k_y^2 v_y^2}}$$



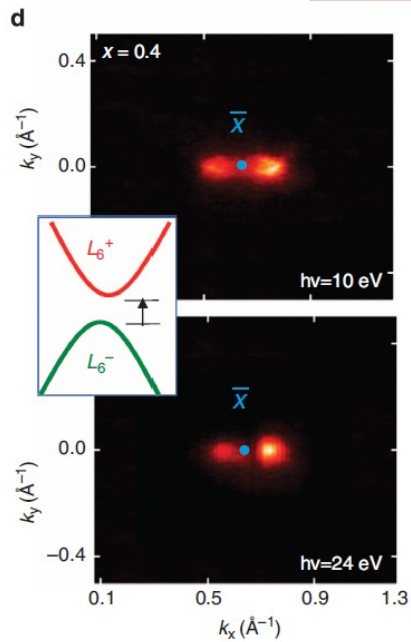
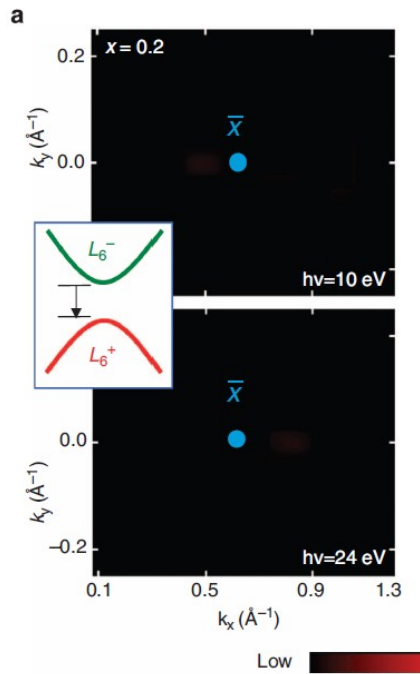
Four bands, the ones closest to  $E=0$  feature Dirac points ( $\bar{\Lambda}_{1,2}$ ) not invariant under time reversal.

Dirac points separated by a pair of 2D Van Hove singularities ( $\bar{S}_{1,2}$ ).

$$\bar{\Lambda}_{1,2} = (0, \pm \sqrt{m^2 + \delta^2}/v_y)$$

$$\bar{S} = (m/v_x, 0)$$

[Liu et al., PRB(R) (2013)]



Observation of surface states  
In the topological crystalline  
Insulator in Pb-SnTe alloy.

[Z. Hasan group, Nature Comm. (2012)]

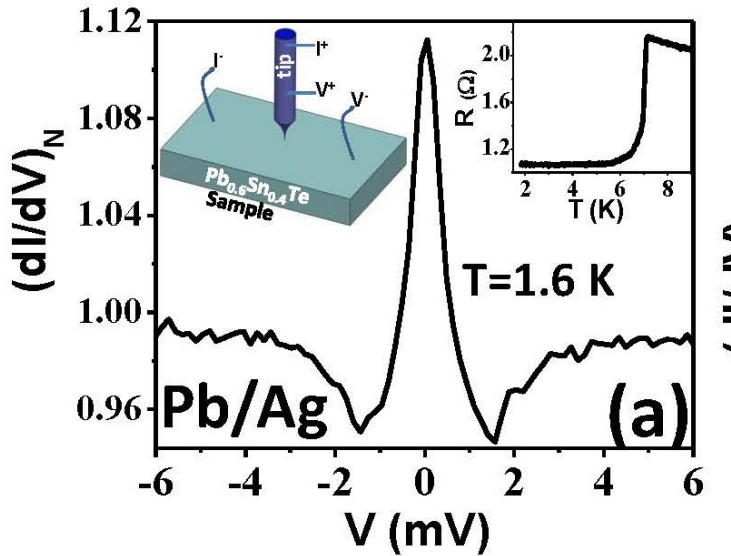
# Electronic instabilities

Essentially spinless bands!

Enhanced DoS at (low-lying!) Van Hove points -> possibility of electronic instabilities if Fermi energy can be tuned to their vicinity through small changes in doping, pressure etc.

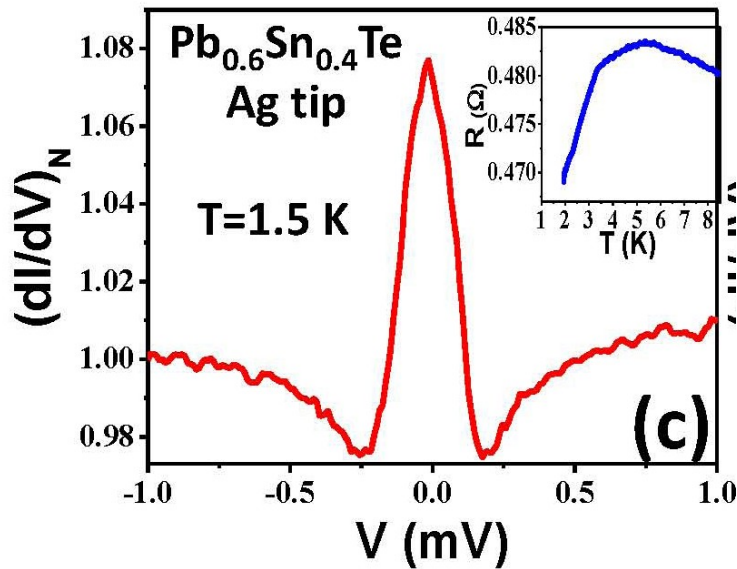
Particularly interested in instabilities from weak repulsive electron interactions. [E.g. Furukawa & Rice, PRL (1998) for d-wave order in cuprates and Nandkishore et al., Nat. Phys. (2012) for chiral d-wave superconductivity in graphene]

Advantage wrt. e.g. graphene [Nandkishore et al., Nat. Phys. (2012)] where 2D Van Hove singularities appear at M points – large doping needed for graphene unlike SnTe.



Experimental evidence for superconductivity in a Pd-Sn-Te alloy.

[G. Sheet group, APL (2016)]



# Model

Particularly interested in instabilities arising from weak repulsive interactions:

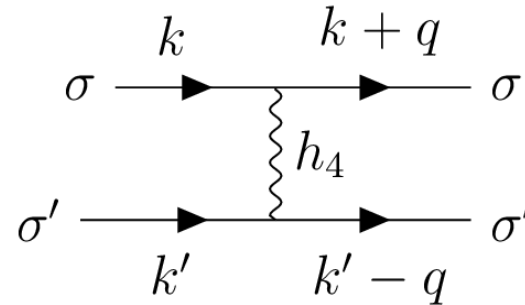
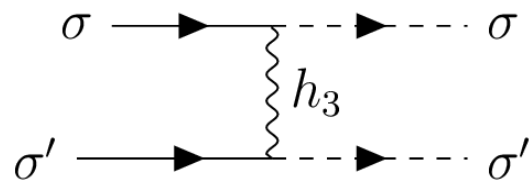
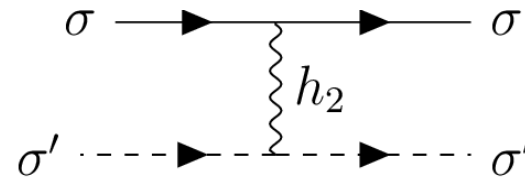
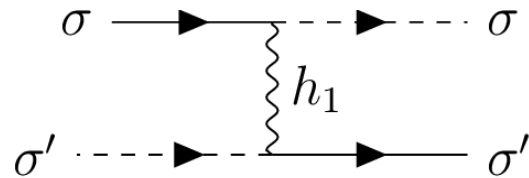
$$L = \sum_{\alpha, \gamma, \gamma'} \left[ \psi_{\alpha}^{\dagger} (\partial_{\tau} - \epsilon_k + \mu) \psi_{\alpha} - \frac{1}{2} h_4^{\gamma\gamma'} \psi_{\alpha}^{\dagger} \psi_{\alpha}^{\dagger} \psi_{\alpha} \psi_{\alpha} \right. \\ \left. - \sum_{\alpha \neq \beta} \frac{1}{2} (h_1^{\gamma\gamma'} \psi_{\alpha}^{\dagger} \psi_{\beta}^{\dagger} \psi_{\alpha} \psi_{\beta} + h_2^{\gamma\gamma'} \psi_{\alpha}^{\dagger} \psi_{\beta}^{\dagger} \psi_{\beta} \psi_{\alpha} \right. \\ \left. + h_3^{\gamma\gamma'} \psi_{\alpha}^{\dagger} \psi_{\alpha}^{\dagger} \psi_{\beta} \psi_{\beta} \right],$$

Sum over patch index  $\alpha$  and spin indices  $\gamma$ .

Multiorbital system: must Allow Hund's splitting of Interactions.

We project the electron fields to the band(s) closest to the chemical potential. Interested in chemical potential in the vicinity of Van Hove singularities (i.e. lowest lying bands).

# ...model



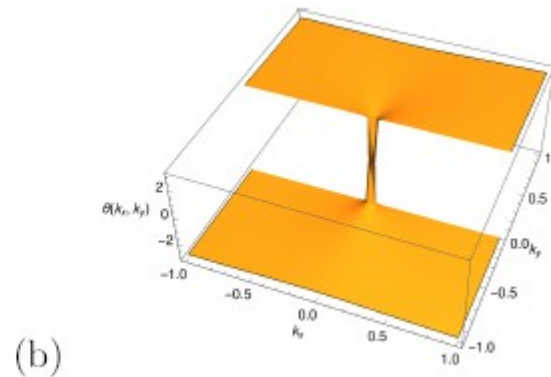
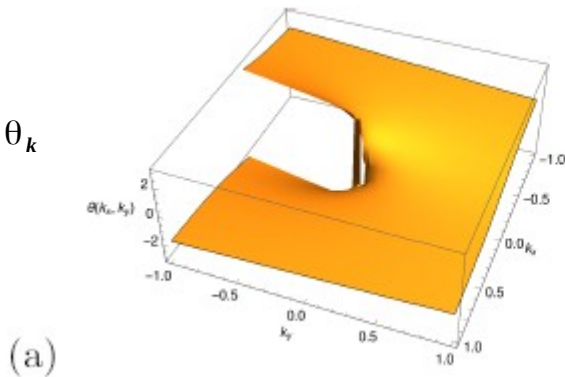
Interactions considered subject to conservation of spin and crystal momentum. The two electron pockets are approximately nested.

# Nontrivial Berry phases

Wavefunctions are four-component spinors. Original electron fields projected to any single wavefunction (say band 1) end up having nontrivial momentum dependences (Berry phases):

$$u_{a\sigma}(\mathbf{k}) = \langle \mathbf{k}, 1 | \psi_{a\sigma}(\mathbf{k}) \rangle$$

$$\text{Arg}[u_{1\uparrow}(\mathbf{k})] \sim e^{i\theta_{\mathbf{k}}}$$



$$\text{Arg}[u_{1\downarrow}(\mathbf{k})]$$

Accordingly, interactions projected to the band also acquire nontrivial Berry phases -> possibility of unconventional electronic order even from momentum independent interactions of the original fermions!

# Parquet analysis

Presence of 2D Van Hove singularities and near-nesting conditions make bare susceptibilities in the particle-particle (pp) channel at zero momentum and particle-hole (ph) channel at the nesting vector doubly logarithmically divergent upon decreasing the energy scale.

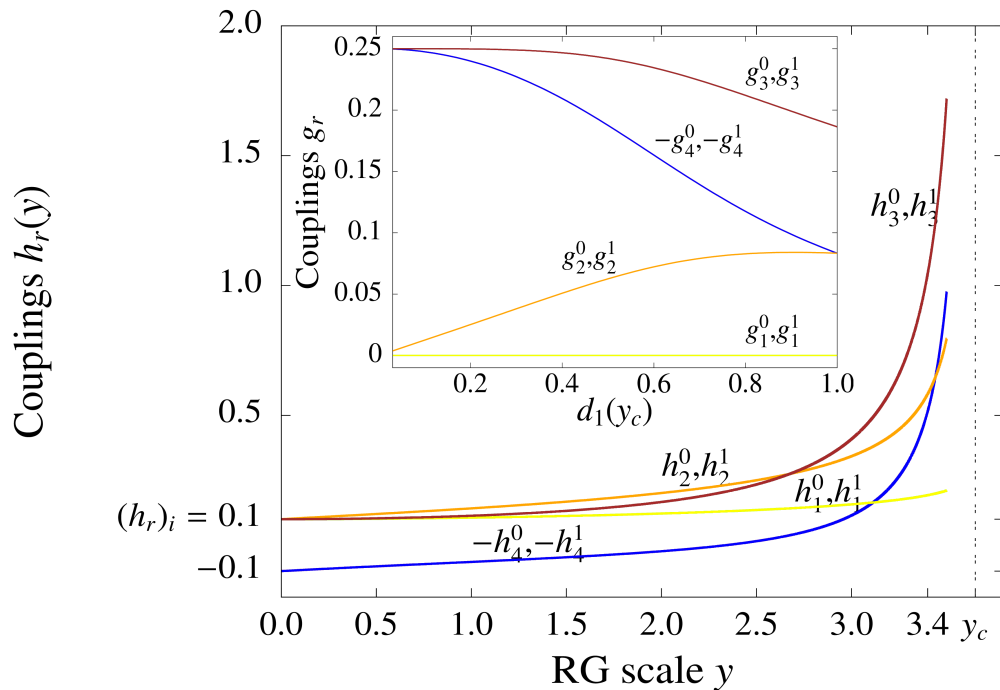
$$\chi_0^{pp}(\omega) \sim \ln[\Lambda/\omega] \ln[\Lambda/\max(\omega, \mu)]$$

$$\chi_Q^{ph}(\omega) \sim \ln[\Lambda/\max(\omega, \mu)] \ln[\Lambda/\max(\omega, \mu, t)]$$

Low energy properties therefore require consideration of competing pp and ph channels. This is the essence of the Parquet approximation.



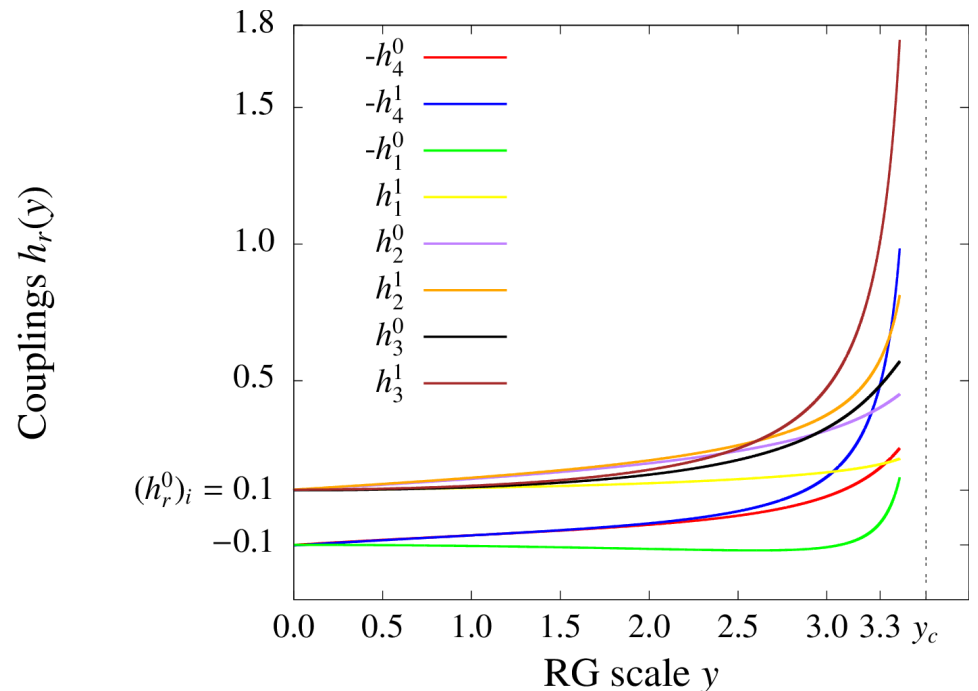
# ... solution of parquet equations



If initial values of couplings are spin-degenerate, the RG flows to spin-degenerate fixed points. Strongest divergence is seen in Pair-hopping ( $h_3$ ) and intra-patch Coulomb ( $h_4$ ).

If spin-antiparallel interaction starts out earlier, then only the  $l=1$  couplings diverge.

Solutions much more sensitive to Hund's splitting than channel splitting.



# Electronic phase competition, susceptibilities

a:

b:

c:

+

d:

+

To study susceptibilities of different orders, we introduce test vertices and consider their renormalization.

E.g. for Cooper pairing on the patch, the order parameters obey

$$\frac{d}{dy} \begin{pmatrix} \Delta_1 \\ \Delta_2 \end{pmatrix} = \begin{pmatrix} 2h_4^{\sigma\bar{\sigma}} & 2h_3^{\sigma\bar{\sigma}} \\ 2h_3^{\sigma\bar{\sigma}} & 2h_4^{\sigma\bar{\sigma}} \end{pmatrix} \begin{pmatrix} \Delta_1 \\ \Delta_2 \end{pmatrix}$$

# Susceptibilities, exponents

Susceptibilities evolve as  $\chi \sim (y_c - y)^\alpha$

$$\alpha_{\text{pw}} = 2(-g_3^{\sigma\bar{\sigma}} + g_4^{\sigma\bar{\sigma}}),$$

$$\alpha_{\text{CDW}} = -2(g_3^{\sigma\bar{\sigma}} - g_1^{\sigma\sigma} - g_1^{\sigma\bar{\sigma}} + g_2^{\sigma\sigma})d_1(y_c),$$

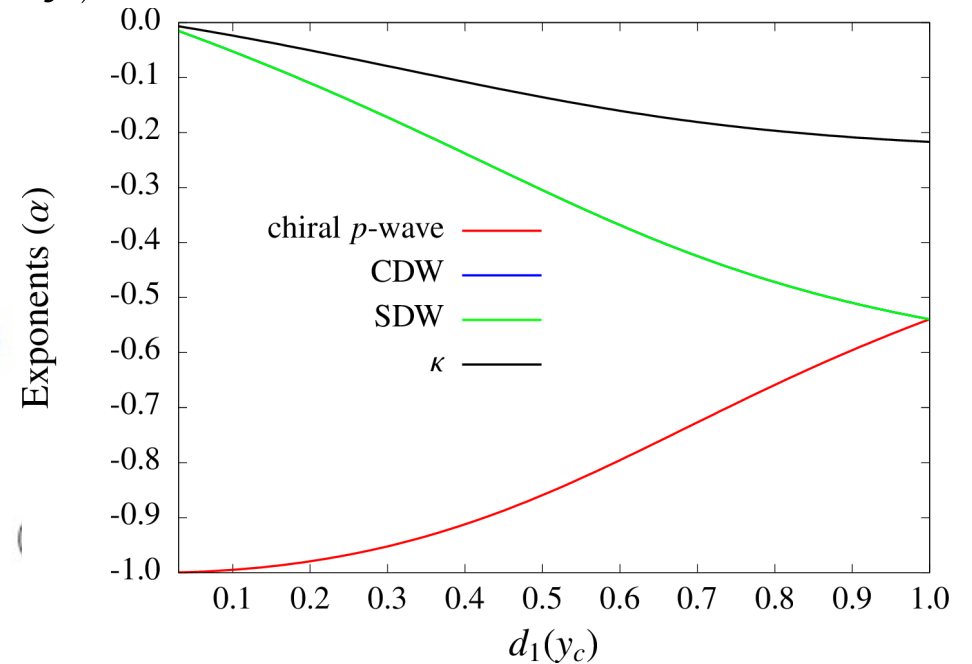
$$\alpha_{\text{SDW}} = -2(g_3^{\sigma\bar{\sigma}} + g_2^{\sigma\bar{\sigma}})d_1(y_c),$$

$$\alpha_\kappa = -2(-g_4^{\sigma\bar{\sigma}} - (g_1^{\sigma\sigma} - g_2^{\sigma\sigma} - g_2^{\sigma\bar{\sigma}}))d_2(y_c),$$

$$\alpha_s = -2(g_4^{\sigma\bar{\sigma}} + g_1^{\sigma\bar{\sigma}})d_2(y_c),$$

$$\alpha_\pi^{\sigma\sigma} = 2(g_2^{\sigma\sigma} - g_1^{\sigma\sigma})d_3(y_c),$$

$$\alpha_\pi^{\sigma\bar{\sigma}} = 2(g_2^{\sigma\bar{\sigma}} - g_1^{\sigma\bar{\sigma}})d_3(y_c).$$



The winner (if one exists) is chiral p-wave superconductivity, which arises from nontrivial Berry phases of the wavefunctions. Translated to original valley-spin basis, the p-wave order is Independent of momentum – hence robust against weak disorder!

# Summary

- 1) Surface states of Pb-doped SnTe are susceptible to electronic instabilities driven by repulsive electron interactions.
- 2) Instabilities very sensitive to exchange splitting of interactions. For dominant antiparallel-spin interactions a chiral p-wave FFLO state is the dominant order. For dominant parallel-spin interaction, there is no phase transition within parquet.
- 3) Chiral p-wave superconductivity arises from nontrivial Berry phases of the surface states, this affords protection against weak potential disorder. Pb-doped SnTe is thus a good candidate to explore chiral p-wave FFLO phases.